

2D In-plane Sensitive Hall Device

Siya Lozanova
 Institute of Robotics
 Bulgarian Academy of Sciences
 Sofia, Bulgaria
 email: lozanovasi@abv.bg

Avgust Ivanov
 Institute of Robotics
 Bulgarian Academy of Sciences
 Sofia, Bulgaria
 email: avgust@ir.bas.bg

Chavdar Roumenin
 Institute of Robotics
 Bulgarian Academy of Sciences
 Sofia, Bulgaria
 email: roumenin@bas.bg

Abstract—A new single-chip silicon 2D in-plane sensitive Hall-effect device having the form of a Greek-cross surrounded by a deep *p*-zone is proposed. In each of the four ends of the *n*-Si cross, one ohmic contact is available. Through the original design and circuitry, two independent currents with non-standard topology sharing the same active region are formed. The contacts are connected to one load resistor each, whereas the resistors with the opposite contacts are fed into one supply terminal, and the resistors with the other two contacts are connected to the other supply terminal. The pairs of opposite contacts are the outputs for the two orthogonal in-plane magnetic-field components at sensitivities $S_{RI} \approx 110$ V/AT. The channel offsets are fully compensated by trimming and the contact numbers are only 4. The non-linearity is small and does not exceed 0.5 % within the range $+ 0.6$ T \div $- 0.6$ T. The cross-talk is very promising and is no more than 2.3% at induction $B = 1.0$ T, the spatial resolution is high compared to the standard solutions, reaching $70 \times 30 \times 40 \mu\text{m}^3$, and the lowest detected magnetic induction with signal - to - noise ratio equal to 1 at supply current of 3 mA is $B_{\text{min}} \approx 11\mu\text{T}$.

Keywords - multidimensional magnetometry; 2D in-plane sensitive Hall device; Lorentz force action; three-contact Hall element; functional integration.

I. INTRODUCTION

The most advanced 2D and 3D vector microsensors are those using the Hall effect principle, since their action involves only one simple and well-defined physical phenomenon. Some of the major advantages are: the position of the multidimensional device with respect to the magnetic source is not as critical as in the case of a 1D sensor, the better orthogonality determined by the planar process, the perfect matching of the channel sensitivities and more. Irrespective of the pronounced progress, these integrated vector transducers feature some essential drawbacks. They have complicated design containing many contacts and numerous connections between them, which restrict fabrication technology and reduce spatial resolution. Another problem is the channel cross-talk and offsets, which impede metrological accuracy. All 2D and 3D Hall devices suffer from these drawbacks [1]–[15]. For example, the contact numbers are 8 – 10 and even more, while the average cross-talk and offsets without compensation reaches around 3.5 - 4 % at induction $B = 1.0$ T and 7-9 mV, respectively. The B_x , B_y and B_z components of field B can be measured via functional integration of orthogonal and in-plane sensitive

Bipolar Magneto Transistors (BMTs) located into a single substrate. Two in-plane differential BMTs with central emitter, a common active region and mutually perpendicular orientations of the other contacts (collectors and bases) are sufficient for the in-plane detection of components B_x and B_y . Unfortunately, the main sensor problems remain, and these are: channel offsets, cross-talk, strong temperature dependence of sensitivities.

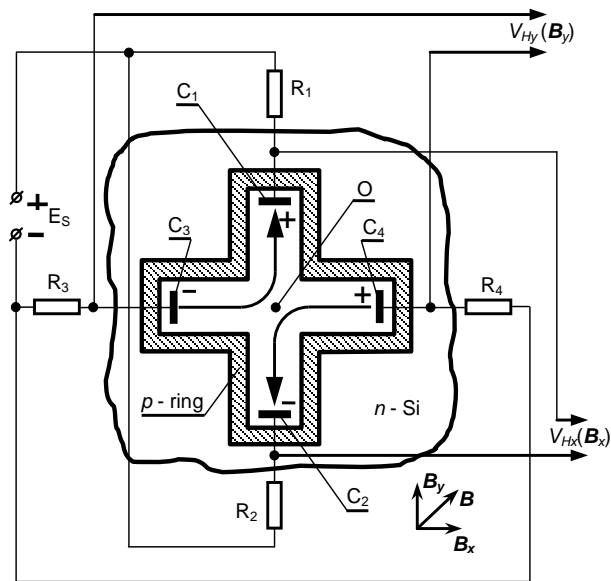


Figure 1. Schematic top-view of silicon 2D integrated Greek-cross Hall device.

The key reason for these drawbacks is the complicated transducer mechanisms acting in the magnetotransistor substrate. That is why the Hall principle of operation remains very frequently used for multidimensional magnetometry. In this paper, we present a novel single-chip sensing device for measurement of two orthogonal in-plane magnetic field components using one and the same transducer region, featuring simple design, high spatial resolution and improved characteristics.

The rest of the paper is structured as follows. In Section II, we present the concept and fabrication of 2D device. In Section III, we show the operating principle, and in Section

IV, we describe the experimental results. We conclude the work in Section V.

II. CONCEPT AND FABRICATION OF THE 2D HALL DEVICE

The new multidimensional device consists of an n -Si Greek-cross surrounded by a deep p -zone. In each end of the cross, symmetrically to its centre O , there is one ohmic n^+ - n contact C_1 , C_2 , C_3 and C_4 , which is connected to one load resistor $R_1 \dots R_4$. Resistors R_1 and R_2 , which are located opposite to contacts C_1 and C_2 , are fed into one terminal of supply E_s , while resistors R_3 and R_4 are connected to the other ends, as shown in Figure 1. The pairs of contacts C_1 - C_2 and C_3 - C_4 are the differential outputs $V_{Hx}(\mathbf{B}_x)$ and $V_{Hy}(\mathbf{B}_y)$ for the two in-plane components \mathbf{B}_x and \mathbf{B}_y of the magnetic-field vector \mathbf{B} .

Notwithstanding the lack of a central supply electrode as with conventional 2D and 3D Hall magnetometers [6]-[9] [11]-[15], through the original design and circuitry, mutually perpendicular current couples I_{C3O} and I_{OC1} , and I_{C4O} and I_{OC2} respectively, are formed, as shown in Figure 1.

The experimental prototype has been implemented using part of the processing steps applied in bipolar Integrated Circuits (IC) technology. The low-doped n -Si plates are 300 μm thick, with resistivity $\rho \approx 7.5 \Omega\cdot\text{cm}$. The carrier's concentration is $n \sim 4.3 \times 10^{15} \text{ cm}^{-3}$. Similar to [17] [18], four masks are employed in the fabrication process. Mask 1 determines the n^+ -implanted zones for ohmic electrical contacts $C_1 \dots C_4$ with the substrate, as the depth of the ohmic n^+ - n junctions is about 1 μm . Mask 2 forms areas for the deep Greek-cross p -ring. The p -ring constricts the effective volume of the sensor and prevents the surface current spreading. All this increases the transducer efficiency of the novel 2D device. Mask 3 defines the metallization layer and bonding pads. Mask 4 is intended for the contact opening in the surface layer SiO_2 for the electrical contact between the metal and the n^+ zones. The width of the deep surrounding p -ring at the surface is about 20 μm (on the mask). The dopant donor concentration of the n^+ - n junctions is $n \approx 10^{20} \text{ cm}^{-3}$. The size of the ohmic contacts $C_1 \dots C_4$ is $20 \times 5 \mu\text{m}^2$, the length and the width of the Greek-cross are 70 μm and 30 μm . The thickness of the effective area is defined in first approximation by the trajectory of currents $I_{C3,C1}$ and $I_{C4,C2}$ penetrating in the n -Si substrate with depth of 30 – 40 μm [15]. As a result, the effective operational volume of the cross is about $70 \times 30 \times 40 \mu\text{m}^3$, which provides high spatial resolution of the new device. The sensor has the following internal resistances: $R_{C1,2} \approx R_{C3,4} \approx 860 \Omega$. Resistors $R_1 \dots R_4$ are at least by one order of magnitude greater than the effective resistance between ohmic contacts $C_1 \dots C_4$, their value being equal to 10 k Ω . At this stage, the 2D in-plane sensitive Hall device is in hybrid realization (resistor elements $R_1 \dots R_4$ are discrete).

III. OPERATING PRINCIPLE

The current paths in the device from Figure 1 start and end on the heavy-doped n^+ contacts $C_1 \dots C_4$. The planar ohmic electrodes $C_1 \dots C_4$ represent equipotential planes to which, in the absence of external magnetic field \mathbf{B} , $B = 0$,

current paths I_{C1} , I_{C2} , and I_{C3} , I_{C4} respectively, flow perpendicularly to the upper surfaces of the n -Si slab, deeply penetrating into the bulk of 30 – 40 μm [15]. The current lines $I_{C1,2}$ and $I_{C3,4}$ in the other parts of the substrate in first approximation are parallel to the upper surface. Therefore, the two trajectories $I_{C1,2}$ and $I_{C4,3}$ are curvilinear. As a result of the uniformity of the structure, as well as of contacts $C_1 \dots C_4$, the two currents components $I_{C1,2}$ and $-I_{C3,4}$ are equal in value and opposite in sign. As a result of technological imperfections, mechanical strain and stress during chip metallization and capsulation, temperature gradients and the like [1] [2] [4] [12] [15] [16], at outputs $V_{Hx}(\mathbf{B}_x = 0)$ and $V_{Hy}(\mathbf{B}_y = 0)$ of the device, at field $B = 0$, offset $V_H(B = 0) \neq 0$ appears, notwithstanding the fact that load resistors $R_1 \dots R_4$ are equal. Full compensation of the offset at the differential channel outputs is carried out by connecting to the load resistors of low-ohmic trimmers. By varying the trimmer values, the offsets vanishes, $V_{Hx}(\mathbf{B}_x = 0) = V_{Hy}(\mathbf{B}_y = 0) = 0$. The original structure from Figure 1 forms, irrespective of the absence of supply electrode in centre O , two identical 3-contact (3C) mutually perpendicular in-plane sensitive Hall devices, possessing two end contacts each, C_1 - C_2 and C_3 - C_4 , [1] [2] [19] [20]. This unexpected solution results from the fact that, with respect to centre O of the cross, current components I_{OC1} and $-I_{OC2}$, and I_{OC3} and $-I_{OC4}$, respectively, feature equal values and opposite directions. The topology of these current paths is the same as in the case where, in centre O , there is a third supply contact. Such innovative structure of the 3C sensor is described for the first time.

In magnetic field \mathbf{B} , $\mathbf{B}_x > 0$ and $\mathbf{B}_y > 0$, the well-known Lorentz force $\mathbf{F}_L = qv_{dr} \times \mathbf{B}_x$ and $\mathbf{F}_L = qv_{dr} \times \mathbf{B}_y$ controls the lateral and vertical components of the drift velocity v_{dr} [1] [2] [19] [20]. In the trajectory parts $O - C_1$ and $O - C_2$, as well as $O - C_3$ and $O - C_4$, respectively, the force \mathbf{F}_L acts in opposite directions. Therefore, the force \mathbf{F}_L shrinks or expands the trajectories towards the surface of the substrate, or towards the bulk. As a result, Hall potential appears on the boundary near to electrodes C_1 and C_2 , and C_3 and C_4 , respectively, and additional (e.g. negative) non-steady-state charges proportional to fields \mathbf{B}_x and \mathbf{B}_y , and current $I_{C1,2}$ arise. Thus, opposite-sign Hall potentials are generated on the respective contacts C_1 - C_2 and C_3 - C_4 . This operation is as in three-contact in-plane sensitive Hall element [19] [20]. Through the circuitry connections, the opposite-sign potentials along the two axes x and y form the respective Hall voltages on the two differential outputs $V_{Hx}(\mathbf{B}_x)$ and $V_{Hy}(\mathbf{B}_y)$ for fields \mathbf{B}_x and \mathbf{B}_y , as shown in Figure 1. Thus, magnetic field \mathbf{B} generates in the x - y plane simultaneously linear and odd output voltages in the channels.

IV. EXPERIMENTAL RESULTS

The output characteristics $V_{Hx}(\mathbf{B}_x)$ and $V_{Hy}(\mathbf{B}_y)$ of the new Greek-cross Hall configuration are presented in Figure 2. The channel sensitivities are equal to $S_{RI} \approx 110\text{V}/\text{AT}$. The non-linearity is small and does not exceed 0.5 % within the range $+ 0.6 \text{ T} \div - 0.6 \text{ T}$. The effective spatial resolution is high, constituting about $70 \times 30 \times 40 \mu\text{m}^3$, which allows to detect more detailed magnetic-field topology.

We realized the measurement of the cross-talk of the 2D device at fixed values of the supply current, $I_s = \text{const}$, after

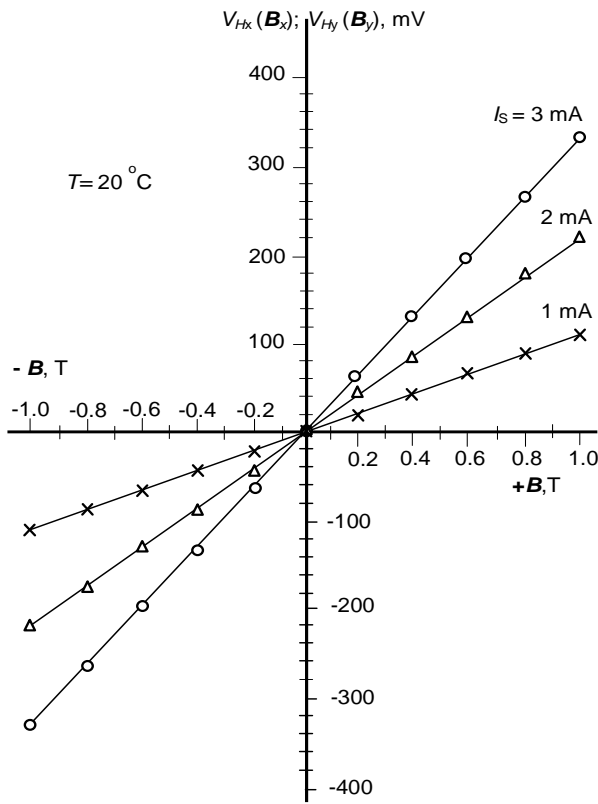


Figure 2. The channel characteristics $V_{Hx}(B_x)$ and $V_{Hy}(B_y)$, offsets are compensated in advance, the current I_s is as a parameter.

the nullification of the two output offsets, using the following approach.

The first step is experimental determination of the channel characteristics of the two outputs – the sensitivity by Hall voltages $V_{Hx}(B_x)$ and $V_{Hy}(B_y)$. The next step is applying homogeneous variable magnetic induction B parallel to one of the axes x or z . The other output (parasitic) the signal from the y -channel is measured.

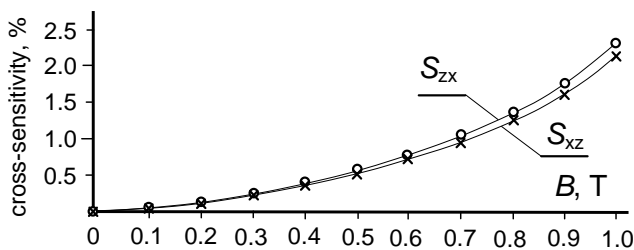


Figure 3. Cross-sensitivity C.S. (cross-talk) of the two-axis device from Figure 1 as a function of induction B , $T = 20^\circ\text{C}$. The cross-talk at induction $B = 1\text{ T}$ reach no more than 2.3 %

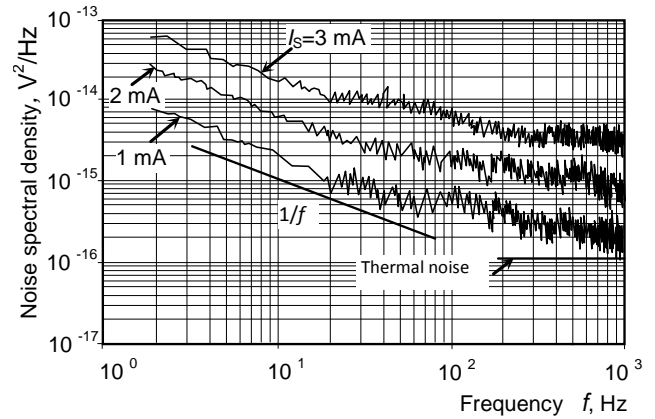


Figure 4. The measured power spectral density of noise of one channel $V_{Hy}(B_y = 0)$ without magnetic field, the supply current I_s is as a parameter, $T = 20^\circ\text{C}$. The noise density for channel $V_{Hx}(B_x = 0)$ is the same.

The procedure described is repeated for the other orthogonal direction x . The cross-sensitivity in our case is mainly due to the geometrical magnetoresistance $MR \sim B^2$, reaching no more than 2.3 % at induction $B \leq 1.0\text{ T}$, as shown in Figure 3. This is a very promising result.

The internal noise of the 2D Hall device without interface circuitry within the range $10\text{ Hz} < f \leq 1\text{ kHz}$ is of the $1/f$ type, as shown in Figure 4. With the increase of bias current I_s , the noise increases, too. The mean lowest detected magnetic induction B_{min} over a $\Delta f = [5\text{ Hz} \div 500\text{ Hz}]$ bandwidth with signal-to-noise ratio $S/N = 1$ at supply current of 3 mA is $B_{\text{min}} \approx 10 - 11\ \mu\text{T}$, where $S_A = \Delta V_H / \Delta B$ is the absolute magnetosensitivity, and $S_{NV}(f)$ is the voltage noise spectral density across the respective output contacts of the new configuration. The induction B_{min} is determined at fully compensated offset in an appropriate magnetic shielded box.

The measured power spectral density of the internal noise in channels $V_{Hx}(B_x)$ and $V_{Hy}(B_y)$ is shown in Figure 4, where the supply current I_s is a parameter at $T = 20^\circ\text{C}$.

The temperature coefficient of the magnetosensitivity reaches about 0.1 %/°C. The established temperature coefficient of the device resistance is $TC_R \approx 0.1\%$.

The thermal behaviour of the fully compensated outputs $V_{Hx}(B_x) = V_{Hy}(B_y) = 0$ at a given temperature T_0 originates from the same active transducer region. In our case, the offset compensation is carried out at $T_0 = 20^\circ\text{C}$. The obtained output voltage-to-residual offset ratio, for example at $T = 40^\circ\text{C}$, reaches about 6×10^3 at induction $B = 1\text{ T}$. This is an optimal result, as shown in Figure 5. With the increase of supply current I_s , as typical for Hall sensors [1] [2], the temperature drift at the output increases. For this reason, a trade-off between drift and sensitivity should be sought. In our case, this situation is achieved at current $I_s \approx 2\text{ mA}$. According to the results, the value of the temperature drift is low. The temperature coefficient of the offset drift reaches no more than 0.1 %/°C.

All measurements of the characteristics of the new 2D device were performed in full compliance with the methodology explained in detail in [1] [2].

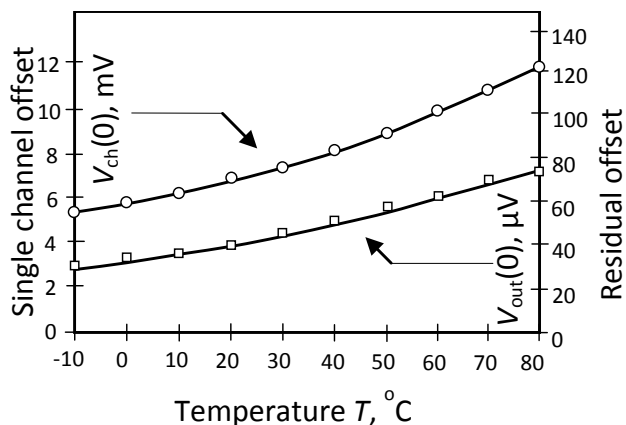


Figure 5. Temperature dependences of the single-channel offset $V_{ch}(0)$ and residual offset $V_{out}(0)$ of the arrangement in Fig. 1, at a supply $I_s = 3$ mA.

V. CONCLUSION

The novel 2D silicon magnetometer for simultaneous measure of two orthogonal components of the magnetic field using a common sensor zone provides good prospects for many applications. Comparing the obtained results with the state-of-the-art shows that the novel 2D Hall sensor possesses at least 15 % better cross-talk, the channel offsets are fully compensated easily by trimming, and the contact numbers are only four. A detailed study of temperature influence on the 2D microsensor characteristics behavior is forthcoming. These results will be used in low-field magnetometry. The fabrication of a fully integrated version of the new 2D sensor is underway. The repeatability of magnetosensitivity and temperature coefficient of sensitivity, in our case, are defined as the maximum variation in the channel output readings when induction B is constant, $B = \text{const}$. At least two calibration cycles are needed [1]. The repeatability of the new device will be determined in the future. The obtained performance is appropriate for contactless applications, such as in robotics and industrial control, tactile systems, space orientation, measurement of angular and linear displacements, speed sensors, end-of-travel transducers, compass, unmanned flight vehicles, navigation, automobiles – ignition timing, Anti-lock Braking System (ABS) systems and more.

ACKNOWLEDGMENT

This work was supported by the National Science Fund at the Ministry of Education and Science of Bulgaria under Project No. DN 07/18-15.12.2016.

REFERENCES

[1] C. Roumenin, Solid State Magnetic Sensors, Elsevier, 1994.
 [2] C. Roumenin, "Microsensors for magnetic field", in MEMS – a practical guide to design, analysis and application, J.G.

Korvink and O. Paul, Eds, Norwich, NY: W. Andrew Publ., pp. 453-521, 2006.
 [3] E. Ramsden, Hall effect sensors – Theory and application, 2nd ed., Elsevier, 2006.
 [4] T. Kaufmann, On the offset and sensitivity of CMOS-based five-contact vertical Hall devices, Der Andere Verlag, Uelvelsbull: MEMS Techn. and Engin., v. 21, 2013.
 [5] M. Demierre, E. Schurig, C. Schott, P. -A. Besse and R. Popovic, "Contactless 360° absolute angular CMOS microsystem based on vertical Hall sensors", Sens. Actuators, v. A 116, pp. 39-44 2004.
 [6] M. Paranjape, L. M. Landsberger and M. Kahrizi, "A CMOS-compatible 2-D vertical Hall magnetic-field sensor using active carrier confinement and post-process micromachining", Sens. Actuators, v. A 53, pp. 278-283, 1996.
 [7] J. Pascal, L. Hebrard, V. Frick and J. P. Blonde, "3D Hall probe integrated in 0.35 um CMOS technology for magnetic field pulses measurements", The Proc. 6th Int. IEEE Northeast Workshop on Circuits and Systems and TAISA Conf., pp. 97-100, 2008.
 [8] L. Franquelo et al. "Three-dimensional space-vector modulation algorithm for four-legmultilevel converters using abc coordinates", IEEE Trans. Ind. Electron. v. 53(2), pp. 458-466, 2006.
 [9] C. -P. Yu, The study and application of a 2D folded Hall sensor chip, Nat. Taipe Univ. of Techn. Publ., p. 88, 2012.
 [10] C. -P. Yu and G. -M. Sung, "Two-dimensional folded CMOS Hall device with interacting lateral magnetotransistor and magnetoresistor", Sens. Actuators, v. A 182, pp. 6-15, 2012.
 [11] C. Wouters et al. "Design and fabrication of an innovative three-axis Hall sensor", Sens. Actuators, v. A 237, pp. 62-71, 2016.
 [12] Ch. S. Roumenin, D. Nikolov and A. Ivanov, "A novel parallel-field Hall sensor with low offset and temperature drift based 2D integrated magnetometer", Sens. Actuators, v. A 115, 303-pp. 307, 2004.
 [13] S. Lozanova, S. Noykov, A. Ivanov, G. Velichkov and C. Roumenin, "3-D silicon Hall device with subsequent magnetic-field components measurement", Procedia Engineering, v. 87, pp. 1107-1110, 2014.
 [14] S. Lozanova, S. Noykov and C. Roumenin, "Three-dimensional magnetometer based on subsequent measurement principle", Sens. Actuators, v. A 248, pp. 281-289, 2016.
 [15] C. Sander, C. Leube and O. Paul, "Three-dimensional magnetometer based on subsequent measurement principle", Sens. Actuators, v. A 222, pp. 329-334, 2015.
 [16] F. Burger, P. -A. Besse and R. S. Popovic, "New fully integrated 3-D silicon Hall sensor for precise angular-position measurements", Sensors and Actuators, v. A 67, pp. 72-76, 1998.
 [17] C. Schott and R. Popovic, "Integrated 3-D Hall magnetic field sensor", The Proc. of Transducers '99, Sendai, Japan, v. 1, pp. 168-171, 1999.
 [18] D. Tanase, Magnetic-based navigation system for endovascular intervention, Grafische Commun. Publ.: Rotterdam, 2003.
 [19] C. Roumenin and P. Kostov, "Planar Hall-effect device", Bulg. patent № BG 37208 B1/26.12.1983.
 [20] S. V. Lozanova and C. S. Roumenin, "Parallel-field silicon Hall effect microsensors with minimal design complexity", IEEE Sensors Journal, v. 9(7), pp. 761-766, 2009.